Journal of Molecular Liquids 387 (2023) 122524

Contents lists available at ScienceDirect

Journal of Molecular Liquids

journal homepage: www.elsevier.com/locate/molliq

Polyether-based ionic liquids from simple mixing of terminal diamines with organic acids to dicationic diammonium carboxylates

Huizhe Liu, Vincent A. Maugein, Georgios Patias, Boyu Zhao, Spyridon Efstathiou, Bryn A. Jones, James Town, Daniel W. Lester, Hannes Houck, David M. Haddleton *

Department of Chemistry, University of Warwick, Gibbet Hill, Coventry CV4 7AL, UK

A B S T R A C T

A new family of dicationic ionic liquids (DIL) have been synthesised by the mixing of either 4,7,10-trioxa-1,13-tridecanediamine or a low molecular weight Jeffamine™ with organic acids such as formic acid, acetic acid, propionic acid, butyric acid, maleic acid, valeric, hexanoic acid, heptanoic acid, benzoic acid and octanoic acid. The structure of the DILs was determined by ^{1}H and ^{13}C NMR and LC-MS. All ILs were soluble in protic polar solvents, especially DMSO, and mostly insoluble in aprotic or non-polar solvents. Thermogravimetric analysis (TGA) and differential scanning calorimetry (DSC) were used to assess the thermal properties of the DILs. Temperature-dependant viscosity and ionic conductivity values were measured at temperatures ranging from 25 to 45 °C. The electrochemical stability of the library of ILs was determined using cyclic voltammetry (CV) with a working electrochemical window of 1.2 V (−0.6 V to 0.6 V).

1. Introduction

Solvents are important in nearly every efficient chemical reactions across all aspects of chemistry [1–3]. Indeed, they are often essential to carry out successful chemical reactions [1]. Volatile organic compounds (VOCs) are commonly used in both laboratory and industrial processes with many advantageous properties, such as the ability to be easily separated from the reaction medium, removal or supply of heat, etc [2]. However, unless these are captured and recycled, the use of VOCs is unsustainable in that they harm the environment due to intrinsic volatility and often toxicity. VOCs can evaporate under ambient conditions resulting in transfer to the environment and atmosphere, producing undesirable photochemical ozone smog which can be carcinogenic and harmful in different ways. Thus, non-volatile solvents are important alternatives [4].

The use of non-volatile ionic liquids as solvents and reagents has expanded in recent years, being reported as being more sustainable with a significant reduction in waste and pollution at both laboratory and industrial scales [5]. Solvents can typically make up to 70 to 80 percent of a process medium [2]. Alternative non-volatile liquids used as solvents are often considered as sustainable, with a reduced/low environmental impact during their full life cycle helping to solve environmental issues while also contributing to overall process optimisation [6,7]. ILs are amongst the most promising candidates for resolving some of the major challenges with regards to chemical pollution. They are often seen as a clean, efficient, and environmentally friendlier alternatives to VOCs, and can offer other substantial benefits due to their excellent thermal, physical and biological capabilities. ILs are sometimes called designer solvents as their properties can be tuned by changing the combination of cations and anions to fit a specific use and tune solubility [2,8]. They have characteristics that adhere to some of the 12 principles of green chemistry. The term environmental factor (E-factor) is a metric to assess how "green" a particular reaction is in terms of waste. The closer to zero the E-factor is, the better. In the case of ILs, E-factor values tend to be near or equal to zero [2,9,10].

ILs are essentially "molten salts" that are typically liquid at temperatures <100 °C and even at ambient temperature [2,11]. Common ILs are a mixture of organic cations, quite often *N* derivatives or *N*'-substituted imidazolium, with organic or inorganic anions (e.g. HSO_4^-) [8,12]. Strong electrostatic interactions between ions provide chemical and thermal stability, solubility in organic and inorganic substances of various polarities, as well as low flammability and insignificant vapour pressure in temperatures below 400 °C [1,13]. They can provide highly viscous solvents in specific chemical reactions [2]. However, in order to generate reliable data for chemical and physical analyses, analytical grade ILs are required [8,14]. Other sustainable advantages of ILs include reduced waste production, facile solvent recovery and reduced environmental emissions [15]. As a result, the use of ILs has expanded in a variety of sectors, including battery technology [16], medicine [17] and solar cells [18]. For example, tetraethylammonium

* Corresponding author.
E-mail address: d.m.haddleton@warwick.ac.uk (D.M. Haddleton).

https://doi.org/10.1016/j.molliq.2023.122524
Received 5 May 2023; Received in revised form 23 June 2023; Accepted 4 July 2023
Available online 14 July 2023

tetrafluoroborate ($Et_4N^+BF_4^-$) in acetonitrile (ACN) is widely utilised in various applications, including in supercapacitors, as a background electrolyte in cyclic voltammetry due to a low viscosity leading to high conductivities. However, it is flammable, very volatile and non-renewable, resulting in environmental pollution [19,20]. ILs have shown excellent performance in clean energy generation reactions, particularly as electrolytes for hydrogen synthesis *via* water electrolysis [21,22]. They have grown in popularity due to their superior thermal stability, low volatility, and fire-retardant properties when compared to organic solvent-based electrolytes [1,23].

There are two main types of ILs: aprotic ILs (APILs) and protic ILs (PILs) [24]. Normally, proton transfer from a Brønsted acid to a Brønsted base produces PILs [25]. These can be inexpensive and easy to synthesise as their synthesis does not result in the formation of by-products [26]. PILs containing a bis(trifluoromethane) sulfonamide anion (TFSI) alongside a range of cations such as alkyl ammonium have been found to be very thermally stable [24,27]. Viscosity and conductivity are important for PILs in many other applications [25,28].

Dicationic ionic liquids (DILs) have received attention in recent years thanks to their increased density of thermal storage, thereby improving charge density and electrostatic energy [29–31]. They have also been reported to be less toxic than monocationic equivalents [32,33]. Recent research has been carried out on the use of anions produced from carboxylates, particularly carboxylic acids, as they can be derived from a wide range of environmentally friendly biological sources [31,34]. For example, a library of dicationic imidazolium-based dicarboxylate ILs was reported by Kuhn *et al.* [31]. Although research on DILs has increased, much of the work so far has focused on imidazolium-based carboxylate ILs. This current work reports on the synthesis, solubility, thermophysical, and electrochemical properties of a new family of polyether-based carboxylate ILs. As these ILs are novel, understanding their properties is essential for potential future applications [31]. Colaino *et al.* have written an in-depth review on poly(ethylene glycol) (PEG)-based ionic liquids as alternative solvents [35]. Many of these PEG-based ILs contain quaternary nitrogen cations, in the form of conventional imidazole units either in between two PEG chains or in the centre of the molecules. We have only found one report of two imidazole units at the two termini of the PEG chain [36], however, these IL are prepared *via* a relatively complex reaction scheme involving three or more steps, using organic solvents which include toluene and ethanol at elevated temperatures, thus impacting the sustainability of the system in its entirety. Indeed, it is often overlooked that the synthesis of ionic liquids uses solvents and temperatures which are counter to the philosophy of Green and Sustainable chemistry. No examples could be found of simple, low molecular weight, PEG-type materials being used to give simple ILs. Herein, we report a family of versatile ionic liquids made from the diamino, short PEG, trioxa-1,13-tridecanediamine with mono acids by either simple mixing, or mixing in water, at room temperature.

2. Results and discussion

2.1. Synthesis

Protic ionic liquids (PILs) were prepared via the stoichiometric combination/mixing of either trioxa-1,13-tridecanediamine or a commercial polyether diamine (Jeffamine D-230, both inexpensive and readily available, with a simple Brønsted acid (Scheme 1). The successful synthesis of a series of ILs derived from trioxa-1,13-tridecanediamine was assessed by monitoring the protonation of the diamine to a diammonium salt through the shift of the amine proton, as well as the disappearance of the acid proton by ^{1}H NMR, with additional evidence provided by Fourier-transform infrared spectroscopy (FT-IR) and LC-MS (p.15–63, ESI). The formation of diamide species following a condensation reaction has been shown by NMR and FT-IR spectroscopy (p77–92, ESI). For example, in the synthesis of [TTDDA][PA], the disappearance of the proton signal (CH_3-CH_2-COO**H**) at 11.9 ppm of propionic acid was monitored, thereby indicating the formation of the propionate (CH_3-CH_2-COO^-) (Fig. S137, ESI). The peak shifting from 1.2 ppm to 6.8 ppm demonstrates that the diamine (H_2N-$(CH_2)_3$-O-$(CH_2)_2$-O-$(CH_2)_2$-O-$(CH_2)_3$-NH_2) was protonated to form a diammonium

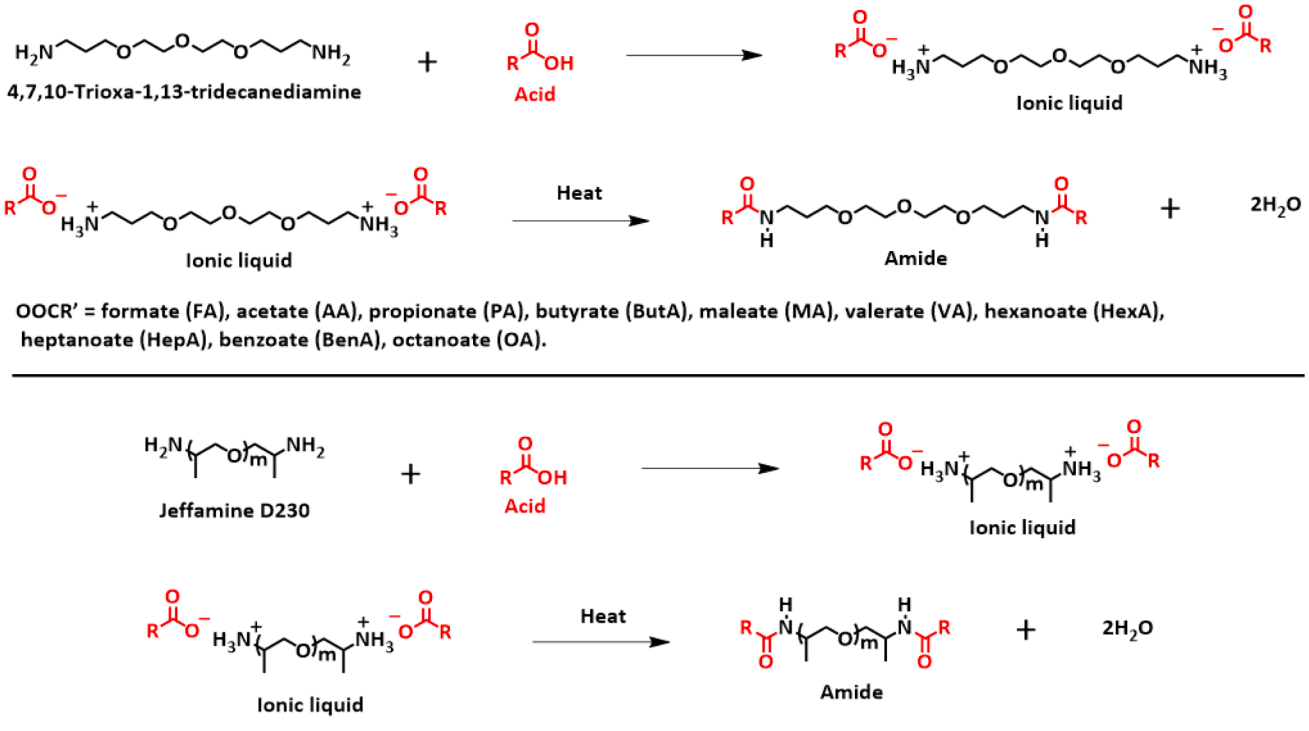

Scheme 1. Synthesis of dicationic polyether-based carboxylate ionic liquids.

salt ($\mathbf{H_3}N^+$-$(CH_2)_3$-O-$(CH_2)_2$-O-$(CH_2)_2$-O-$(CH_2)_3$-$N^+\mathbf{H_3}$). Water used in the synthesis of ILs was removed in *vacuo* and the residual water content determined by by Karl-Fisher titration. It was found to be easier to remove water from ILs with saturated anions when the alkyl chain length was increased (Table 1). Heating of 4,7,10-trioxa-1,13-tridecanediammonium propionate ([TTDDA][PA]) at 220 °C for 6 h led to the intramolecular condensation of the PIL to form a diamide, as observed by ^{1}H NMR (Fig. S138, ESI). The peak from the diammonium salt (δ = 6.8 ppm) shifts with the formation of the diamide (δ = 7.8 ppm) on reaction completion. FT-IR data supports successful synthesis of the amide (Fig. S139, ESI). The $\nu_{N\text{-}H}$ of the amine is shown by the weak broad band at 3410 cm^{-1}. After heating, certain bands in the FT-IR support amide formation, such as the medium sharp band and strong sharp bands at 3298 cm^{-1} and 1632 cm^{-1}, assigned to amide A and amide I, respectively. Four additional ILs were made using a commercial polyether diamine (Jeffamine D-230) and various organic acids: acetic acid, propionic acid, heptanoic acid and octanoic acid. Their thermal phase-change behaviour was compared to that of ILs made with trioxa-1,13-tridecanediamine. The successful synthesis of Jeffamine D-230-based ILs was assessed by monitoring the shift of the diamine proton at 1.4 ppm to approximately 8 ppm, indicative of diammonium salt formation. FT-IR and LC-MS analyses were also conducted (p64–76, ESI).

Table 1
Denomination, water content and physical appearance of the ILs.

Ionic liquid	Abbreviation	Physical appearance	Karl-Fisher Titration (%)
4,7,10-Trioxa-1,13-tridecanediammonium formate	[TTDDA][FA]	Colourless liquid	1.84
4,7,10-Trioxa-1,13-tridecanediammonium acetate	[TTDDA][AA]	Viscous pale yellow liquid	1.83
4,7,10-Trioxa-1,13-tridecanediammonium propionate	[TTDDA][PA]	Viscous pale yellow liquid	1.83
4,7,10-Trioxa-1,13-tridecanediammonium butyrate	[TTDDA][ButA]	Viscous pale yellow liquid	1.83
4,7,10-Trioxa-1,13-tridecanediammonium maleate	[TTDDA][MA]	Viscous colourless liquid	1.81
4,7,10-Trioxa-1,13-tridecanediammonium valerate	[TTDDA][VA]	Viscous pale yellow liquid	1.44
4,7,10-Trioxa-1,13-tridecanediammonium hexanoate	[TTDDA][HexA]	Viscous pale yellow liquid	0.79
4,7,10-Trioxa-1,13-tridecanediammonium heptanoate	[TTDDA][HepA]	Viscous pale yellow liquid	0.41
4,7,10-Trioxa-1,13-tridecanediammonium benzoate	[TTDDA][BenA]	Viscous colourless liquid	1.83
4,7,10-Trioxa-1,13-tridecanediammonium octanoate	[TTDDA][OA]	Viscous pale yellow liquid	0.57

Table 2
Solubility of ILs in common solvents.

	Water	2,2,2-Trifluoroethanol (TFE)	Methanol	Ethanol	Dimethyl sulfoxide (DMSO)	Dimethylformamide (DMF)	Acetone	Dichloromethane (DCM)	Chloroform	Tetrahydrofuran (THF)	Toluene	Hexane
Good solubility												
Medium solubility												
Poor solubility												
[TTDDA][FA]							●	●	●	●	●	●
[TTDDA][AA]							●			●	●	●
[TTDDA][PA]										●	●	●
[TTDDA][ButA]										●	●	●
[TTDDA][MA]							●	●	●	●	●	●
[TTDDA][VA]										●	●	●
[TTDDA][HexA]											●	●
[TTDDA][HepA]												●
[TTDDA][BenA]							●			●	●	●
[TTDDA][OA]												●

2.2. Solubility

The solubility of these ILs in commonly used solvents was evaluated. Common representative organic solvents were selected with a range of relative polarities. These include water: 1.00; TFE: 0.90; methanol: 0.76; ethanol: 0.65; DMSO: 0.44; DMF: 0.39; Acetone: 0.35; DCM: 0.31; Chloroform: 0.25; THF: 0.21; Toluene: 0.10 and Hexane: 0.01 [37]. Each IL was dissolved in 0.1 g amounts and was given the following solubility ratings: good when soluble in 1 mL of the solvent, medium when soluble in 3 mL of the solvent, and poor when insoluble in 3 mL at 25 °C and ambient pressure [31]. The ILs were generally more soluble in solvents with higher relative polarity such as water and methanol (Table 2). Low solubility was observed in aprotic polar solvents (acetone, chloroform) and nonpolar solvents (toluene, hexane), whereas DMSO was miscible with all ILs. The presence of the anionic carboxylate group of the ILs facilitates their miscibility in polar protic solvents [31]. Additionally, increasing the length of the alkyl group increased solubility, with [TTDDA][HepA] and [TTDDA][OA] being soluble in the widest range of solvents. The presence of double bonds ([TTDDA][MA]) or ring structures ([TTDDA][BenA]) in the ILs led to poorer solubility compared to linear, saturated analogues ([TTDDA][ButA] and [TTDDA][HepA]).

2.3. Thermal stability

The thermal stability of an IL is an important parameter for many applications [38,39]. Several factors can affect the thermal stability of ILs including cation modification, as well as cation and anion types [40]. In the present case, the anion is a carboxylate with an alkyl chain length ranging from one to eight carbons. The onset temperature (T_{on}), obtained from thermogravimetric analysis (TGA), is taken as the thermal decomposition temperature of the IL [31,38–40]. The TGA traces of the ILs (Fig. 1, Table 3) show T_{on} across a range of 30 °C to 600 °C with more

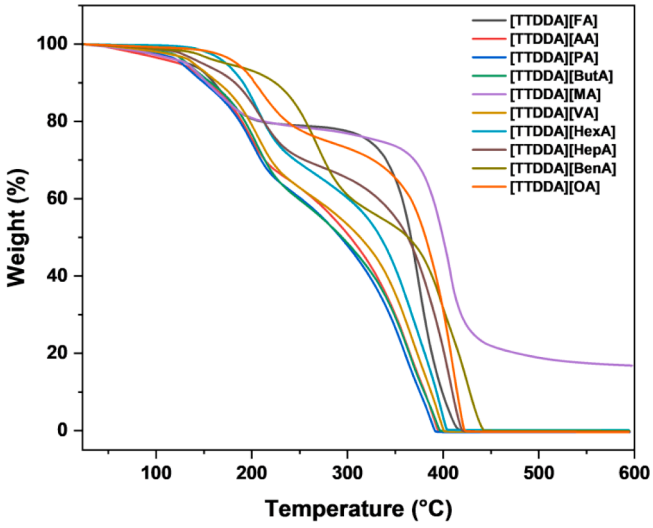

Fig. 1. TGA graphs of ILs, under N_2, from 30 to 600 °C at 10 K/min in 90 µl alumina pans.

Table 3
Degradation steps data of the TGA graphs in Fig. 1.

Ionic liquid	Mass loss step	Degradation temperature T_{on} (°C)	Weight (%)
[TTDDA][FA]	1	145	18
	2	348	70
[TTDDA][AA]	1	172	29
	2	329	65
[TTDDA][PA]	1	177	34
	2	323	63
[TTDDA][ButA]	1	186	32
	2	331	61
[TTDDA][MA]	1	132	18
	2	381	62
[TTDDA][VA]	1	180	30
	2	338	64
[TTDDA][HexA]	1	173	32
	2	348	67
[TTDDA][HepA]	1	183	26
	2	369	72
[TTDDA][BenA]	1	237	36
	2	385	60
[TTDDA][OA]	1	180	23
	2	377	76

Table 4
DSC data for the ILs, under N_2, from −100 to 220 °C at 10 K/min in an aluminium pan.

Ionic liquid	1st heating cycle T_g (°C)	2nd heating cycle				
		T_g (°C)	T_c (°C)	ΔH_c (J/g)	T_m (°C)	ΔH_m (J/g)
[TTDDA][FA]	−75	−66	N/A	N/A	N/A	N/A
[TTDDA][AA]	−55	−64	N/A	N/A	N/A	N/A
[TTDDA][PA]	−69	−65	N/A	N/A	N/A	N/A
[TTDDA][ButA]	−70	−75	N/A	N/A	N/A	N/A
[TTDDA][MA]	−66	−8	N/A	N/A	N/A	N/A
[TTDDA][VA]	−70	−69	9	26	51	25
[TTDDA][HexA]	−70	−73	−19	140	56	188
[TTDDA][HepA]	−62	−76	−27	14	63	43
[TTDDA][BenA]	−54	−23	N/A	N/A	N/A	N/A
[TTDDA][OA]	−62	N/A	N/A	N/A	7; 72	9; 33
[JEFFAMINE][AA]	−37	−52	N/A	N/A	N/A	N/A
[JEFFAMINE][PA]	−36	−63	N/A	N/A	N/A	N/A
[JEFFAMINE][HepA]	−64	−51	N/A	N/A	N/A	N/A
[JEFFAMINE][OA]	−57	−56	N/A	N/A	N/A	N/A

than one apparent decomposition step. TGA-mass spectrometry analysis suggests the first mass loss step is due to water evaporation arising from the formation of the amide species, as well as the degradation of the acid backbone resulting in the formation of alkyl fragments (Fig. S142, ESI).

Taking the second T_{on} as the main thermal degradation step, following amide formation, it was observed that increasing the alkyl chain of the anion resulted in a decrease in thermal stability from [TTDDA][FA] to [TTDDA][PA]. On the other hand, increasing the alkyl chain length, from [TTDDA][ButA] to [TTDDA][OA] led to higher IL thermal stability thanks to the lower hydrophilicity of the anion, (Fig. 1, Table 3). Based on their T_{on}, it is evident that the IL of a saturated anion ([ButA]) is less thermally stable than its unsaturated analogue ([MA]). Additionally, the thermostability of the IL can be enhanced by substituting the linear anion ([HepA]) with one containing an aromatic ring ([BenA]) (Fig. 1, Table 3).

2.4. Thermal phase-change behaviour

Glass transition temperatures (T_g) were determined by differential scanning calorimetry (DSC) [31]. All of the ILs synthesized in this work experienced solid–liquid and liquid–solid transitions (Table 4), suggesting these ILs displayed both an amorphous and crystalline phase (p.15–76, ESI, for DSC curves). In the case of [TTDDA][HexA] (Fig. 2), the first heating cycle revealed a T_g at −70 °C (heating rate of 10 °K/min) with a water loss step between 120 and 220 °C indicating the condensation reaction of [TTDDA][HexA] to the diamide. The phase change to the diamide is seen through the shift of the T_g −73 °C on the second heating cycle, as well as the observation of both crystallisation and melting point peaks.

All ILs (Table 4) showed a T_g during the first heating cycle only, which suggests that the material is amorphous [41]. Since diamides produced as a result of the second heating cycle do not reflect the properties of the ILs, only the T_g obtained during the first heating cycle was used to compare the thermal phase-change behaviour of the different ILs [TTDDA][FA] exhibited the lowest T_g (−75 °C), whereas [TTDDA][AA] showed the highest T_g (−55 °C) of all the ILs with linear saturated anions. The T_g of the ILs can be increased either by substitution of ([ButA]) with an unsaturated anion ([MA]) or by using one with an aromatic ([BenA]) rather than linear ([HepA]) structure (Table 4). A lower T_g is expected to lead to favourable physicochemical features such as low viscosity and increased ionic conductivity [41]. Following the removal of water produced by the condensation reaction and formation of the diamide species, two behaviours were observed in the second heating cycle. Firstly, ILs exhibiting a glass transition showed that the diamide remained amorphous. This behaviour corresponds to ILs [TTDDA][FA] through [TTDDA][MA] as well as [TTDDA][BenA]. The second behaviour, exhibited in diamides formed by [TTDDA][VA], [TTDDA][HexA] and [TTDDA][HepA], displayed a glass transition, crystallisation, and subsequent melting temperature. The family of ILs synthesized with Jeffamine D-230, exhibited thermal properties similar to ILs made with trioxa-1,13-tridecanediamine. It was noted that there are many different, commercially available, polyether amines which should show similar behaviour (Table 4).

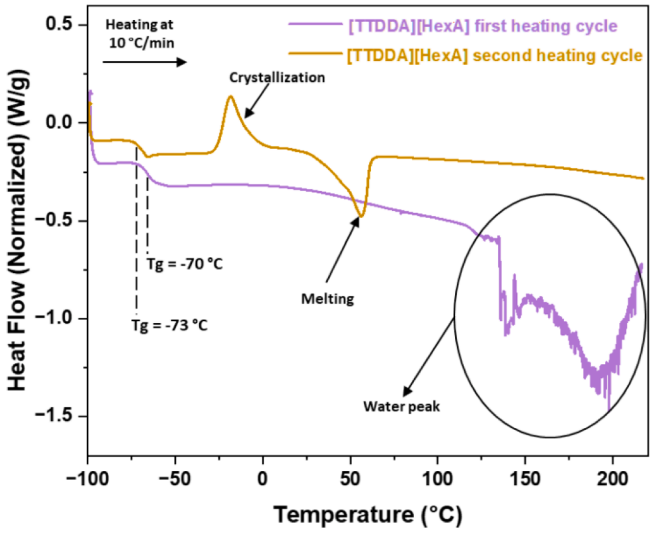

Fig. 2. DSC of [TTDDA][HexA], under N_2, from −100 to 220 °C at 10 K/min in an aluminium pan.

2.5. Shear viscosity dependence on temperature

Viscosity was measured between 25 °C and 45 °C (Table 5) [41]. Each IL showed Newtonian behaviour within this temperature range

Table 5
Average viscosity (η) of ILs at 25 °C, 35 °C and 45 °C at a shear rate of 25 S^{-1}.

Temperature	25 °C	35 °C	45 °C
Ionic liquid	**Average viscosity (mPa·s)**		
[TTDDA][FA]	360.2 ± 27.2	235.3 ± 3.9	171.1 ± 3.8
[TTDDA][AA]	3800.7 ± 245.8	1929.8 ± 22.7	1227.3 ± 40.4
[TTDDA][PA]	1599.7 ± 69.9	993.1 ± 20.2	629.5 ± 35.9
[TTDDA][ButA]	1139.9 ± 26.4	780.3 ± 25.2	523.6 ± 39.3
[TTDDA][MA]	6132.4 ± 898.2	2785.5 ± 295.7	1448.2 ± 200.4
[TTDDA][VA]	5448.3 ± 564.8	2522.0 ± 80.5	1683.3 ± 40.0
[TTDDA][HexA]	6162.1 ± 521.6	3321.5 ± 211.9	1853.2 ± 84.6
[TTDDA][HepA]	6227.4 ± 633.2	3262.2 ± 259.6	1858.9 ± 38.1
[TTDDA][BenA]	15945.7 ± 3013.1	8013.4 ± 2316.4	3120.7 ± 550.5
[TTDDA][OA]	6569.5 ± 754.3	3070.0 ± 309.4	1814.7 ± 69.2

(Figures S140, S141, ESI). The decrease in viscosity with increasing temperature is in agreement with Khan *et al.* [41]. Fig. 3. The viscosities for [TTDDA][ButA], [TTDDA][MA], [TTDDA][HepA], [TTDDA][BenA] were 1140, 6132, 6227, and 15940 mPa·s at 25 °C respectively (Table 5). Analogues with linear monoanions, [TTDDA][MA] and [TTDDA][BenA] displayed higher viscosities. An increase in the alkyl chain length did not directly correlate with a specific trend in viscosity [42].

The activation energy (E_η) of the ILs was determined using a plot of ln η vs. 1/T (Fig. 4 and Table S145, ESI) [TTDDA][MA] and [TTDDA][BenA] showed higher E_η values, presumably due to stronger electrostatic interactions between their anions and cations [43]. The estimated E_η values for the ILs synthesized in this work ranged from 12 to 28 KJ·mol^{-1}, which was relatively lower than those of dicationic imidazolium-based ILs obtained in previous research (43 to 78 KJ·mol^{-1}) [41].

2.6. Conductivity dependence on temperature

Ionic conductivity is determined by viscosity, the degree of ion dissociation, ionic charge, and ion mobility. This property is of major importance for many applications [44]. The ionic conductivity of trioxa-1,13-tridecanediamine-based ILs was measured at 25 °C, 35 °C and 45 °C, where values between 6.64 × 10^{-3} to 2.98 mS.cm^{-1} were measured (Fig. 5, Table 6). It was observed that conductivity values increased slightly as temperature increased. Varying the chain length of the anion did not significantly affect conductivity, however, it varied considerably when rigidity was introduced into the anion structure. For example, when the anion was changed from [ButA] to [MA], the

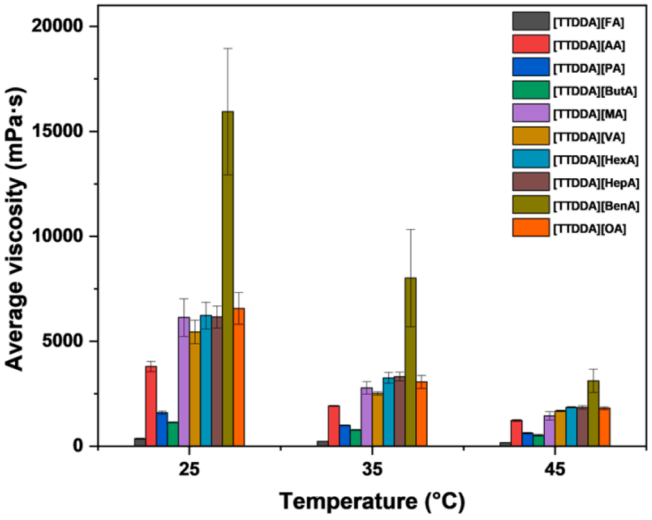

Fig. 3. Average viscosity (η) of ILs at 25 °C, 35 °C and 45 °C at a shear rate of 25 S^{-1}.

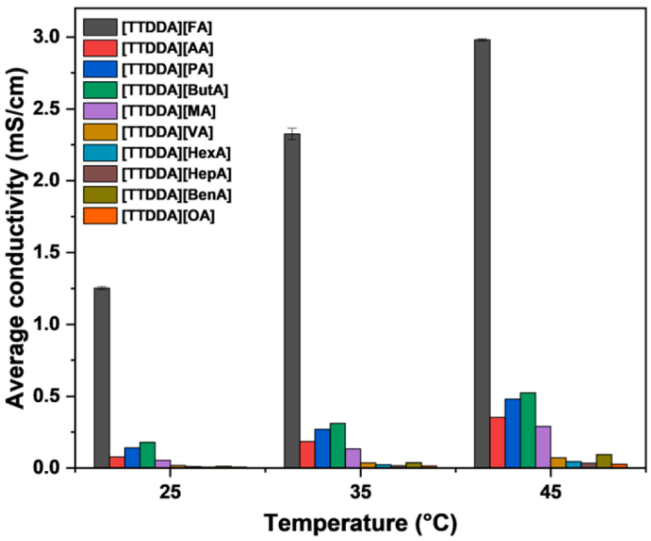

Fig. 4. Viscosity (η) as a function of temperature for the ILs studied in this work.

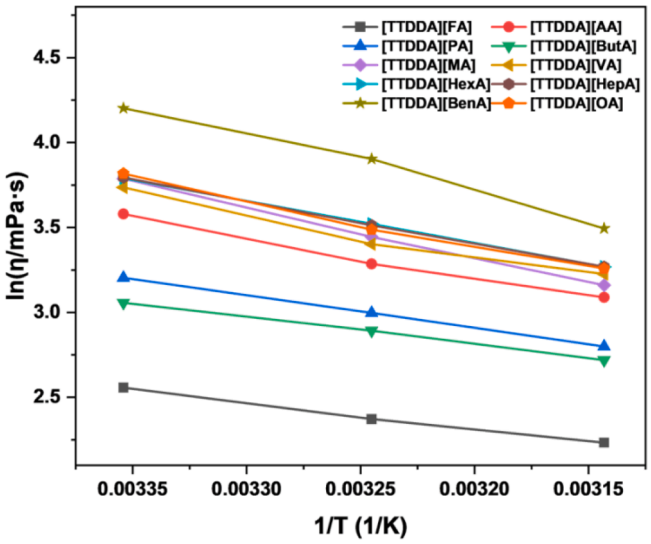

Fig. 5. Average conductivity of ILs at 25 °C, 35 °C and 45 °C.

conductivity decreased from 0.18 to 5.31 × 10^{-2} mS.cm^{-1}, at 25 °C. Conductivity followed the Arrhenius equation in logarithmic form, $\ln\lambda = \ln\lambda_0 + E_a/RT$, with E_a and λ_0 the activation energy of conductivity and limiting conductivity, respectively, in the temperature range of 25 to 45 °C (Fig. 6 and Table S146, ESI). Ionic conductivity in ILs showed a weaker dependence on the alkyl length of the anion whilst exhibiting stronger dependency on structural changes such as the presence of unsaturated double bonds or aromatic rings [TTDDA][FA] displayed the highest ionic conductivity, with 1.25 mS.cm^{-1} at 25 °C (Table 6). In general, the series of ILs with the lowest viscosity hadthe highest ionic conductivity, which is consistent with earlier studies by Greaves *et al.* [45].

2.7. Electrochemical stability

The electrochemical stability of the ILs was investigated by cyclic voltammetry (CV) [46] with a working electrochemical window of 1.2 V (−0.6 V to 0.6 V, vs. Ag/AgCl) in the presence of potassium ferricyanide ($K_3Fe(CN)_6$) [47]. Water as a solvent was used as reference. In order to counteract the high viscosity and hygroscopic nature of the ILs, the

Table 6
Average conductivity of ILs at 25 °C, 35 °C and 45 °C.

Temperature	25 °C	35 °C	45 °C
Ionic liquid	**Average conductivity (mS/cm)**		
[TTDDA][FA]	$1.25 \pm 1.06 \times 10^{-2}$	$2.33 \pm 4.03 \times 10^{-2}$	$2.98 \pm 8.16 \times 10^{-3}$
[TTDDA][AA]	$7.71 \times 10^{-2} \pm 5.25 \times 10^{-4}$	$0.18 \pm 5.44 \times 10^{-4}$	$0.35 \pm 8.16 \times 10^{-4}$
[TTDDA][PA]	$0.14 \pm 1.79 \times 10^{-3}$	$0.27 \pm 4.47 \times 10^{-4}$	$0.48 \pm 8.16 \times 10^{-4}$
[TTDDA][ButA]	$0.18 \pm 7.79 \times 10^{-4}$	$0.31 \pm 1.10 \times 10^{-4}$	$0.52 \pm 8.16 \times 10^{-4}$
[TTDDA][MA]	$5.31 \times 10^{-2} \pm 4.97 \times 10^{-4}$	$0.13 \pm 4.71 \times 10^{-5}$	$0.29 \pm 1.25 \times 10^{-3}$
[TTDDA][VA]	$1.74 \times 10^{-2} \pm 1.15 \times 10^{-4}$	$3.61 \times 10^{-2} \pm 8.16 \times 10^{-5}$	$7.24 \times 10^{-2} \pm 4.71 \times 10^{-5}$
[TTDDA][HexA]	$1.09 \times 10^{-2} \pm 8.16 \times 10^{-6}$	$2.29 \times 10^{-2} \pm 4.71 \times 10^{-5}$	$4.55 \times 10^{-2} \pm 1.25 \times 10^{-4}$
[TTDDA][HepA]	$7.66 \times 10^{-3} \pm 1.70 \times 10^{-5}$	$1.67 \times 10^{-2} \pm 2.94 \times 10^{-5}$	$3.34 \times 10^{-2} \pm 1.25 \times 10^{-4}$
[TTDDA][BenA]	$1.19 \times 10^{-2} \pm 1.44\ 10^{-4}$	$3.82 \times 10^{-2} \pm 4.71 \times 10^{-5}$	$9.29 \times 10^{-2} \pm 9.20 \times 10^{-4}$
[TTDDA][OA]	$6.64 \times 10^{-3} \pm 2.16 \times 10^{-5}$	$1.14 \times 10^{-2} \pm 3.09 \times 10^{-5}$	$2.74 \times 10^{-2} \pm 4.71 \times 10^{-5}$

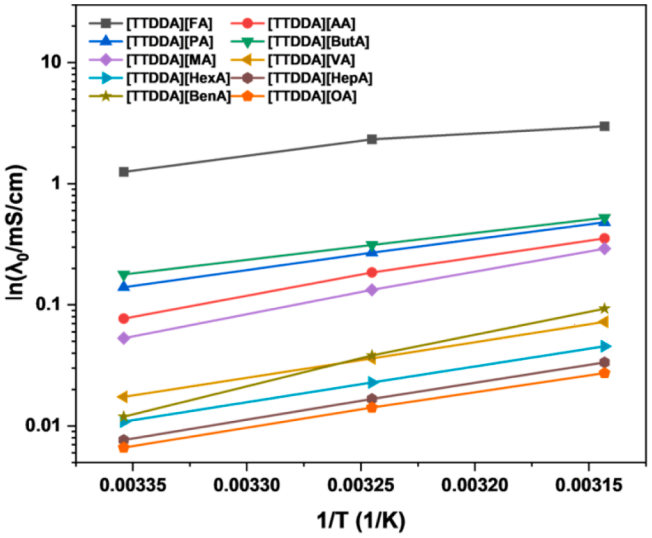

Fig. 6. Conductivity as a function of temperature for the ILs studied in this work.

electrochemical cell was kept at 358 K during the experiment (Fig. 7 and p. 15–63, ESI). In the case of [TTDDA][MA], as the scan rate was increased from 0.05 to 0.4 V/s (−0.6 V to 0.6 V, vs. Ag/AgCl), the reduction peak ($E_{p,c}$) became more negative and the cathodic peak current rose (Fig. 7). Peak separation ($\Delta E = E_{p,a} - E_{p,c}$) was found to be 0.090 V at 0.05 V/s, with the value increasing with higher scan rates. On the other hand, the average peak potential ($E_{1/2} = (E_{p,c} + E_{p,a})/2$) remained constant at all scan rates (Fig. 7, Table 7). Overall, when compared to water as a solvent, ILs showed relatively lower ΔE over four different scan rates (Fig. S143, Table S147, ESI).

In all cases, as the scan rate was increased, the reduction and oxidation peak potentials moved increasingly apart, with ($E_{p,c}$) shifting to a more negative potential and ($E_{p,a}$) increasing. These results demonstrate that the Fe(III)/Fe(II) reduction in an IL medium at a GC electrode is quasi-reversible and governed by both charge transfer and diffusion processes [47]. The Randles-Sevcik equation (1) can be used to calculate the diffusion coefficient for electrochemically reversible electron transfer processes that involve freely diffusing redox species such as Fe(III)/Fe(II) when applied to a quasi-reversible system [46–48]

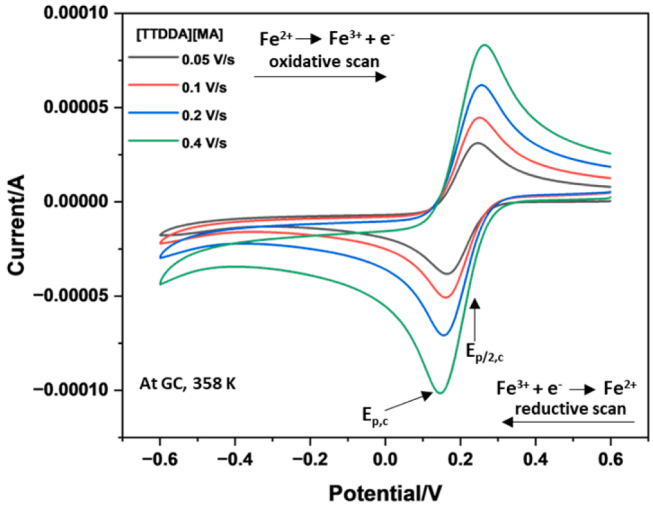

Fig. 7. Cyclic voltammograms of 50 mM Fe(III) in [TTDDA][MA] at a glassy carbon electrode at various scan rates at 358 K.

Table 7
Data obtained from the cyclic voltammograms of Fe(III)/Fe(II) reversible couple in [TTDDA][MA] at a glassy carbon electrode at 358 K.

v (V/s)	$E_{p,c}$ (V)	$E_{p,a}$ (V)	$E_{1/2}$ (V)	ΔE (V)
0.05	0.161	0.251	0.206	0.090
0.1	0.155	0.255	0.205	0.100
0.2	0.151	0.257	0.204	0.106
0.4	0.139	0.267	0.203	0.128

$$i_{p,c} = 0.446nFAC^{o}\left(\frac{nFvD_o}{RT}\right)^{\frac{1}{2}} \quad (1)$$

where $i_{p,c}$ (A) is the cathodic peak current, n is the number of electrons transferred in the redox event, F (C/mol) is the Faraday constant, A (cm^2) is the electrode surface area, C^0 is the concentration of Fe(III) ion (mol/cm^3), v (V/s) is the scan rate, D_o (cm^2/s) is the diffusion coefficient, R (J/K/mol) is the gas constant and T (K) is the absolute temperature. The diffusion coefficient at 358 K of each IL can be found in Table S148 (ESI). Cathodic peak current ($i_{p,c}$) increased with increasing scan rate (v). Faster scan rates caused a reduction in the size of the diffusion layer, resulting in higher currents [46]. The Randles-Sevcik

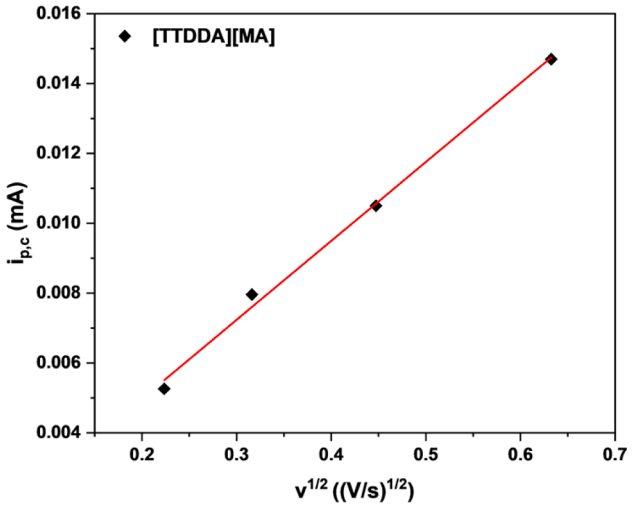

Fig. 8. Plot of $i_{p,c}$ versus $v^{1/2}$ of [TTDDA][MA].

equation also illustrates how cathodic peak current ($i_{p,c}$) increases linearly with the square root of the scan rate ($v^{1/2}$). Fig. 8 shows the plot of $i_{p,c}$ against $v^{1/2}$, which is linear. The anodic and cathodic limits were measured at a scan rate of 0.1 V/s in order to investigate the stability of these ILs for electrochemical applications. Increasing the alkyl chain length of linear saturated anions gradually increased the electrochemical window (Fig. S144, Table S149, ESI). The IL [TTDDA][OA], having the anion with the longest chain length, provided the widest electrochemical window, ranging from −2.49 V to 2.00 V (vs. Ag/AgCl).

3. Conclusions

We report a family of ten new dicationic ionic liquids (DILs) with protonated trioxa-1,13-tridecanediamine as dication, in addition to four DILs with a poly(ether amine) of nominal molecular weight 270 $g.mol^{-1}$ with different simple anions. They were synthesised through simple mixing of inexpensive reagents and were analysed using ^{1}H and ^{13}C NMR as well as LC-MS. The DILs showed a large temperature window where they remained as free flowing ionic liquids, however, upon heating in excess of approximately 120 °C they underwent a condensation reaction to form diamides, with further thermal degradation at higher temperatures. Replacing a linear chain anion with one with an aromatic ring or one with an unsaturated double bond such as maleate enhanced both the thermostability and glass transition temperature of the IL. The solubility of ILs in common organic solvents has been evaluated, with low solubility observed in aprotic polar solvents (acetone, chloroform) and nonpolar solvents (toluene, hexane) but good solubility in polar solvents such as DMSO thanks to the anionic carboxylate group. It was also established that whilst viscosity decreased with increasing temperature, ionic conductivity increased as well. Cyclic voltammograms showed that the reduction of Fe(III)/Fe(II) in IL electrolytes was quasi-reversible and regulated by both charge transfer and diffusion processes. Furthermore, it was verified that the cathodic peak current ($i_{p,c}$) increased linearly with the square root of the scan rate ($v^{1/2}$). These simple to prepare and low-cost ionic liquids show potential to be introduced in place of existing materials in diverse applications.

Declaration of Competing Interest

The authors declare that they have no known competing financial interests or personal relationships that could have appeared to influence the work reported in this paper.

Data availability

Data will be made available on request.

Acknowledgements

We thank the Research Technology Platforms (RTP) of the University of Warwick and Dr Daniel Lester as well as Dr James Town for providing training and equipment as well as EPSRC, United Kingdom for equipment funded in part by EPSRC EP/V036211/1 and EP/V007688/1. H.A. H. acknowledges funding of his EUTOPIA-SIF fellowship received from the European Union's Horizon 2020 research and innovation programme under the Marie Skłodowska-Curie grant agreement No. 945380.

Appendix A. Supplementary material

Supplementary data to this article containing experimental details, intrumentation details, additional viscosity, conductive, and thermal data can be found online at https://doi.org/10.1016/j.molliq.2023.122524.

References

[1] S.S. de Jesus, R. Maciel Filho, Renew. Sustain. Energy Rev. 157 (2022), 112039.
[2] V. Hessel, N.N. Tran, M.R. Asrami, Q.D. Tran, N. Van Duc Long, M. Escribà-Gelonch, J.O. Tejada, S. Linke, K. Sundmacher, Green Chem. 24 (2022) 410–437.
[3] P. Lozano, J.M. Bernal, S. Nieto, C. Gomez, E. Garcia-Verdugo, S.V. Luis, Chem. Commun. 51 (2015) 17361–17374.
[4] P.G. Jessop, Green Chem. (2011) 13.
[5] M. Vert, Y. Doi, K.-H. Hellwich, M. Hess, P. Hodge, P. Kubisa, M. Rinaudo, F. Schué, Pure Appl. Chem. 84 (2012) 377–410.
[6] C. Capello, U. Fischer, K. Hungerbühler, Green Chem. (2007) 9.
[7] P.G. Jessop, Faraday Discuss. 206 (2018) 587–601.
[8] S.K. Singh, A.W. Savoy, J. Mol. Liq. (2020) 297.
[9] M. Deetlefs, K.R. Seddon, Green Chem. 12 (2010) 17–30.
[10] A. DeVierno Kreuder, T. House-Knight, J. Whitford, E. Ponnusamy, P. Miller, N. Jesse, R. Rodenborn, S. Sayag, M. Gebel, I. Aped, I. Sharfstein, E. Manaster, I. Ergaz, A. Harris, L. Nelowet Grice, A.C.S. Sustainable, Chem. Eng. 5 (2017) 2927–2935.
[11] H. Ohno, Electrochemical Aspects of Ionic Liquids, Wiley Online Library, 2011.
[12] L.V.N.R. Ganapatibhotla, J. Zheng, D. Roy, S. Krishnan, Chem. Mater. 22 (2010) 6347–6360.
[13] M.-L.-C.-J. Moita, Â.F.S. Santos, J.F.C.C. Silva, I.M.S. Lampreia, J. Chem. Eng. Data 57 (2012) 2702–2709.
[14] A. Stark, P. Behrend, O. Braun, A. Müller, J. Ranke, B. Ondruschka, B. Jastorff, Green Chem. (2008) 10.
[15] P.L. Amado Alviz, A.J. Alvarez, J. Clean. Prod. 168 (2017) 1614–1624.
[16] Y. Domi, H. Usui, N. Ieuji, K. Nishikawa, H. Sakaguchi, ACS Appl. Mater. Interfaces 13 (2021) 3816–3824.
[17] M.D.T. Torres, S. Voskian, P. Brown, A. Liu, T.K. Lu, T.A. Hatton, C. de la Fuente-Nunez, ACS Nano 15 (2021) 966–978.
[18] A. Wang, X. Deng, J. Wang, S. Wang, X. Niu, F. Hao, L. Ding, Nano Energy (2021) 81.
[19] T. Abdallah, D. Lemordant, B. Claude-Montigny, J. Power Sources 201 (2012) 353–359.
[20] B. Zhao, M. Mohammed, B.A. Jones, P. Wilson, Chem. Commun. 57 (2021) 3897–3900.
[21] M.P. Stracke, G. Ebeling, R. Cataluna, J. Dupont, Energy Fuels 21 (2006) 1695–1698.
[22] C. Acar, I. Dincer, J. Clean. Prod. 218 (2019) 835–849.
[23] D. Kuang, C. Klein, Z. Zhang, S. Ito, J.E. Moser, S.M. Zakeeruddin, M. Gratzel, Small 3 (2007) 2094–2102.
[24] T.L. Greaves, C.J. Drummond, Chem. Rev. 108 (2008) 206–237.
[25] K. Ghandi, Green Sustain. Chem. 04 (2014) 44–53.
[26] H. Markusson, J.P. Belieres, P. Johansson, C.A. Angell, P. Jacobsson, Chem. A Eur. J. 111 (2007) 8717–8723.
[27] S. Nazari, S. Cameron, M.B. Johnson, K. Ghandi, J. Mater. Chem. A (2013) 1.
[28] A. Davoodnia, M.M. Heravi, Z. Safavi-Rad, N. Tavakoli-Hoseini, Synth. Commun. 40 (2010) 2588–2597.
[29] H. Zhang, W. Xu, J. Liu, M. Li, B. Yang, J. Mol. Liq. 282 (2019) 474–483.
[30] H. Zhang, J. Liu, M. Li, B. Yang, J. Mol. Liq. 269 (2018) 738–745.
[31] B.L. Kuhn, B.F. Osmari, T.M. Heinen, H.G. Bonacorso, N. Zanatta, S.O. Nielsen, D.T. S. Ranathunga, M.A. Villetti, C.P. Frizzo, J. Mol. Liq. (2020) 308.
[32] M.G. Montalbána, G. Vílloraa, P. Licenceb, Ecotoxicol. Environ. Saf. 150 (2018) 129–135.
[33] C. Xu, Z. Cheng, Processes (2021) 9.
[34] C. Florindo, F.S. Oliveira, L.P.N. Rebelo, A.M. Fernandes, I.M. Marrucho, ACS Sustain. Chem. Eng. 2 (2014) 2416–2425.
[35] M.M. Cecchini, C. Charnay, F. De Angelis, F. Lamaty, J. Martinez, E. Colacino, ChemSusChem 7 (2014) 45–65.
[36] L. Wang, Y. Zhang, C. Xie, Y. Wang, Synlett 34 (2005) 1861–1864.
[37] A.I. Vogel, A.R. Tatchell, B.S. Furniss, A.J. Hannaford, P.W.G. Smith, Vogel's Textbok of Practical Organic Chemistry, 5th ed., Pearson, 1996.
[38] K. Oster, P. Goodrich, J. Jacquemin, C. Hardacre, A.P.C. Ribeiro, A. Elsinawi, J. Chem. Thermodyn. 121 (2018) 97–111.
[39] X. Lin, R. Kavian, Y. Lu, Q. Hu, Y. Shao-Horn, M.W. Grinstaff, Chem. Sci. 6 (2015) 6601–6606.
[40] Y. Cao, T. Mu, Ind. Eng. Chem. Res. 53 (2014) 8651–8664.
[41] A.S. Khan, Z. Man, A. Arvina, M.A. Bustam, A. Nasrullah, Z. Ullah, A. Sarwono, N. Muhammad, J. Mol. Liq. 227 (2017) 98–105.
[42] Z. Ullah, M.A. Bustam, Z. Man, N. Muhammad, A.S. Khan, RSC Adv. 5 (2015) 71449–71461.
[43] J.F. Kincaid, H. Eyring, A.E. Stearn, Chem. Rev. 28 (1941) 301–365.
[44] M.A. Susan, A. Noda, S. Mitsushima, M. Watanabe, Chem. Commun. (2003) 938–939.
[45] T.L. Greaves, A. Weerawardena, C. Fong, I. Krodkiewska, C.J. Drummond, J. Phys. Chem. B 110 (2006) 22479–22487.
[46] N. Elgrishi, K.J. Rountree, B.D. McCarthy, E.S. Rountree, T.T. Eisenhart, J. L. Dempsey, J. Chem. Educ. 95 (2017) 197–206.
[47] K. Shakeela, A.S. Dithya, C.J. Rao, G.R. Rao, J. Chem. Sci. 127 (2015) 133–140.
[48] R. Nagaishi, M. Arisaka, T. Kimura, Y. Kitatsuji, J. Alloy. Compd. 431 (2007) 221–225.